12th International Symposium on Turbulence and Shear Flow Phenomena (TSFP12)
Osaka, Japan (Online), July 19-22, 2022

SCALE-DEPENDENT GEOMETRIC STATISTICS OF THE LAGRANGIAN AND EULERIAN ACCELERATIONS IN HOMOGENEOUS TURBULENT SHEAR FLOW

Frank G. Jacobitz
Department of Mechanical Engineering, University of San Diego
5998 Alcalá Park, San Diego, CA 92110, USA
jacobitz@sandiego.edu

Kai Schneider
Institut de Mathématiques de Marseille (I2M), Aix-Marseille Université, CNRS
39 rue Joliot-Curie, 13453 Marseille cedex 13, France
kai.schneider@univ-amu.fr

ABSTRACT

The alignment properties of different vector-valued flow quantities, including the Lagrangian, Eulerian, and convective accelerations in homogeneous turbulent shear flow, are quantified through the introduction of scale-dependent geometrical statistics. The vector fields are decomposed into an orthogonal wavelet series and the angles of the scale-wise contributions of different vector-valued flow quantities can be determined. This approach allows us to revisit the random Taylor hypothesis by examining the cancellation properties of Eulerian and convective accelerations at different flow scales. The results for homogeneous turbulent shear flow, computed by direct numerical simulation, show that Taylor's hypothesis holds at small scales of the flow as reflected by the anti-alignment of the Eulerian acceleration and the convective term. Such anti-alignment, however, is not observed at the largest scales of the turbulent motion, indicating that Taylor's hypothesis does not generally hold for homogeneous turbulent shear flow.

INTRODUCTION

Taylors frozen-ow hypothesis (Taylor, 1938) supposes that small-scale eddies in turbulent ows move downstream at a constant speed with little distortion. Temporal and spatial fluctuations in turbulent flows can thus be related, and, for example, temporal spectra in experimental measurements can be converted into spatial spectra. Hot-wire measurements in turbulent flows often implicitly assume its validity. Theoretically, it is also of utmost importance to understand convection in turbulent flows and the related temporal to spatial intermittency. Moreover, both play an important role in two-point closure turbulence models for space-time correlations in Eulerian and Lagrangian reference frames (He *et al.*, 2017). However, Taylor's hypothesis has many limitations, such as the requirements of weak shear rates and low turbulence intensities. Discussions on its validity have a long history and are still subject to some controversy in the recent literature (e.g., Moin, 2009; Del Alamo & Jiménez, 2009).

Motivated by the random Taylor hypothesis or sweeping decorrelation hypothesis, stating that 'small eddies in turbulent flow being swept past a stationary Eulerian observer,' (cf. Tennekes, 1975) acceleration fluctuations and their different contributions have been studied in Pinsky *et al.* (2000) and Tsinober *et al.* (2001) for isotropic turbulence. Their work is based on the prediction of Tennekes (1975), which states that the Lagrangian acceleration must be small, justified by the consideration of Eulerian and Lagrangian time scales.

Homogeneous turbulent shear flow has been investigated as a prototypical example of turbulence due to the importance of shear production in the geophysical environment and in many engineering applications. In homogeneous flows, the statistical properties of turbulence do not change in the spatial directions (x, y, and z), but they evolve in time t. While this simplification has been used extensively as the basis of numerical simulations, homogeneous turbulent shear flow was first studied experimentally. Rose (1966) and Champagne *et al.* (1970) are credited with the first experimental studies of homogeneous turbulent shear flow. Rohr *et al.* (1988) established that the eventual evolution of homogeneous turbulent shear flow follows an exponential growth law. Using direct numerical simulations, Jacobitz *et al.* (1997) confirmed the exponential evolution and also investigated the impact of buoyancy forces on the flow. This prototypical flow has been studied extensively including the effects of buoyancy and rotation as well as using a variety of statistical methods (e.g., Salhi *et al.*, 2014).

Motivated by our recent work in Jacobitz & Schneider (2021), in which we studied the Lagrangian and Eulerian acceleration properties of fluid particles in homogeneous turbulence with uniform shear and uniform stable stratification, we generalize this approach here to investigate scale dependent geometrical statistics. A wavelet-based scale-dependent decomposition of the Lagrangian and Eulerian accelerations is performed and the alignment properties are analyzed at different scales of the turbulent motion (e.g., Farge & Schneider, 2015). The aim of this work is to address the applicability of Taylor's hypothesis at small scales in homogeneous turbulent shear flow.

The remainder of the manuscript first presents the numerical approach based on direct numerical simulations. Then, Lagrangian and Eulerian accelerations are introduced, their corresponding orthogonal wavelet decomposition is presented,

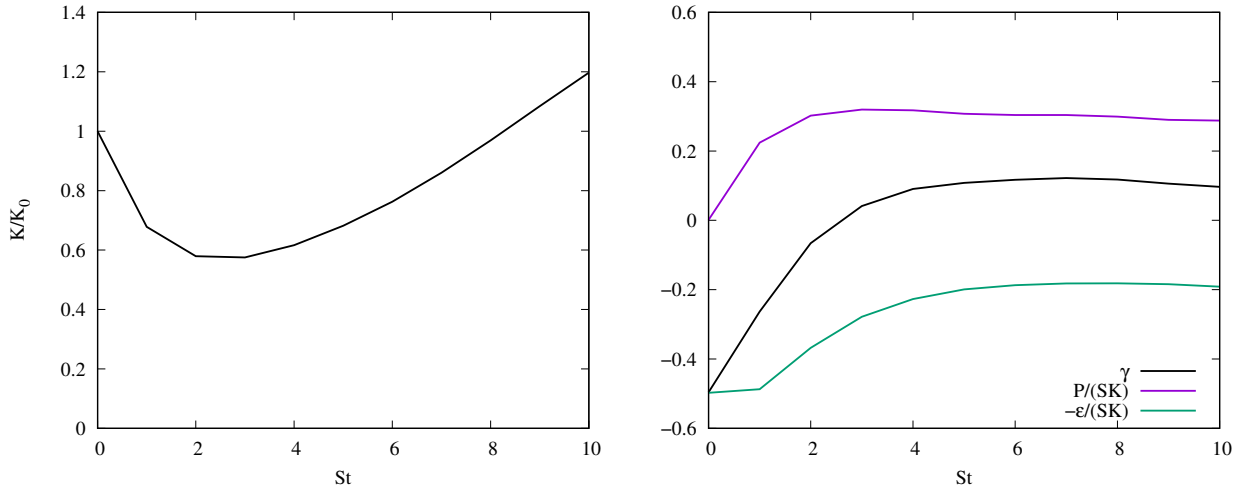

Figure 1. Evolution of the normalized turbulent kinetic energy K/K_0 with normalized time St (left) as well as the growth rate of the turbulent kinetic energy γ, the normalized production rate $P/(SK)$, and the normalized dissipation rate $\varepsilon/(SK)$ (right).

and the scale-dependent alignment of Eulerian and convective accelerations are considered. Results illustrate our findings, considering the direct numerical simulation data of turbulent homogeneous shear flow, and conclusions complete the manuscript.

NUMERICAL APPROACH

The present study is based on a direct numerical simulation of homogeneous turbulent shear flow using the incompressible form of the Navier-Stokes equations for the fluctuating components of velocity and pressure with an imposed constant vertical shear rate $S = \partial U/\partial y$. The equations of motion are transformed into a frame of reference moving with the mean velocity (Rogallo, 1981). This transformation enables the application of periodic boundary conditions for the fluctuating components of velocity and pressure. A spectral collocation method is used for the spatial discretization and the solution is advanced in time with a fourth-order RungeKutta scheme. The simulations are performed using 512^3 grid points. The initial conditions are taken from a separate simulation of isotropic turbulence, which was allowed to develop for approximately one eddy turnover time. The initial value of the Taylor-microscale Reynolds number is $Re_\lambda = 89$ and $SK/\varepsilon = 2$ for the shear number. The corresponding values at $St = 10$ are $Re_\lambda = 157$ and $SK/\varepsilon = 5.22$. The results are analyzed at $St = 10$.

SCALE-DEPENDENT STATISTICS

The Lagrangian and Eulerian accelerations $\boldsymbol{a}_L = \boldsymbol{a}_E + \boldsymbol{a}_C$, where $\boldsymbol{a}_C$ denotes the convective contribution, are defined as

$$\boldsymbol{a}_L = \frac{\partial \boldsymbol{u}}{\partial t} + \boldsymbol{u}\cdot\nabla\boldsymbol{u} \quad \text{and} \quad \boldsymbol{a}_E = \frac{\partial \boldsymbol{u}}{\partial t}, \tag{1}$$

respectively. Both accelerations are computed as a volume average at a fixed time, which is an appropriate choice for homogeneous flows. The effect of shear is considered as an external force. The pressure-gradient term is given by $\boldsymbol{a}_P = \boldsymbol{\nabla}(p/\rho_0)$, where ρ_0 is the ambient density.

For defining scale-dependent alignment statistics of the above quantities, we use a three-dimensional orthogonal vector-valued wavelet decomposition. To this end we consider a generic vector field $\boldsymbol{a} = (a_1, a_2, a_3)$ at a fixed time instant and decompose each component $a_\alpha(\boldsymbol{x})$ into an orthogonal wavelet series,

$$a_\alpha(\boldsymbol{x}) = \sum_\lambda \widetilde{a}^\alpha_\lambda \, \psi_\lambda(\boldsymbol{x}), \tag{2}$$

where the wavelet coefficients are given by the scalar product $\widetilde{a}^\alpha = \langle a_\alpha, \psi_\lambda \rangle$ (e.g., Farge & Schneider, 2015). The wavelets ψ_λ with the multi-index $\lambda = (j, \boldsymbol{i}, d)$ are well localized in scale $L_0 2^{-j}$ (where L_0 corresponds to the size of the computational domain), around position $L_0\boldsymbol{i}/2^j$, and orientated in one of the seven directions $d = 1, \ldots, 7$, respectively. Reconstructing the three components a_α at scale $L_0 2^{-j}$ by summing only over the position $\boldsymbol{i}$ and direction d indices in eq. (2) yields the vector field $\boldsymbol{a}^j$ at scale index j. By construction we have $\boldsymbol{a} = \sum_j \boldsymbol{a}^j$, where the $\boldsymbol{a}^j$ are mutually orthogonal.

The scale-dependent statistical moments of the flow fields, including scale-dependent flatness, and scale-dependent pdfs, can thus be computed from $\boldsymbol{a}^j$ using classical statistical estimators. For instance, the q-th order moment of $\boldsymbol{a}^j(\boldsymbol{x})$ can be defined by,

$$M_q[\boldsymbol{a}^j] = \langle (\boldsymbol{a}^j)^q \rangle, \tag{3}$$

and by construction the mean value vanishes with $\langle \boldsymbol{a}^j \rangle = 0$. The moments are thus central moments. These scale-dependent moments are directly related to the q-th order structure functions (Schneider *et al.*, 2004), where the increment size is $\propto 2^{-j}$.

The scale-dependent flatness, which measures the intermittency of $\boldsymbol{a}^j$ at scale 2^{-j}, is defined by

$$Fl[\boldsymbol{a}^j] = \frac{M_4[\boldsymbol{a}^j]}{(M_2[\boldsymbol{a}^j])^2}. \tag{4}$$

For a Gaussian distribution the flatness equals three at all scales.

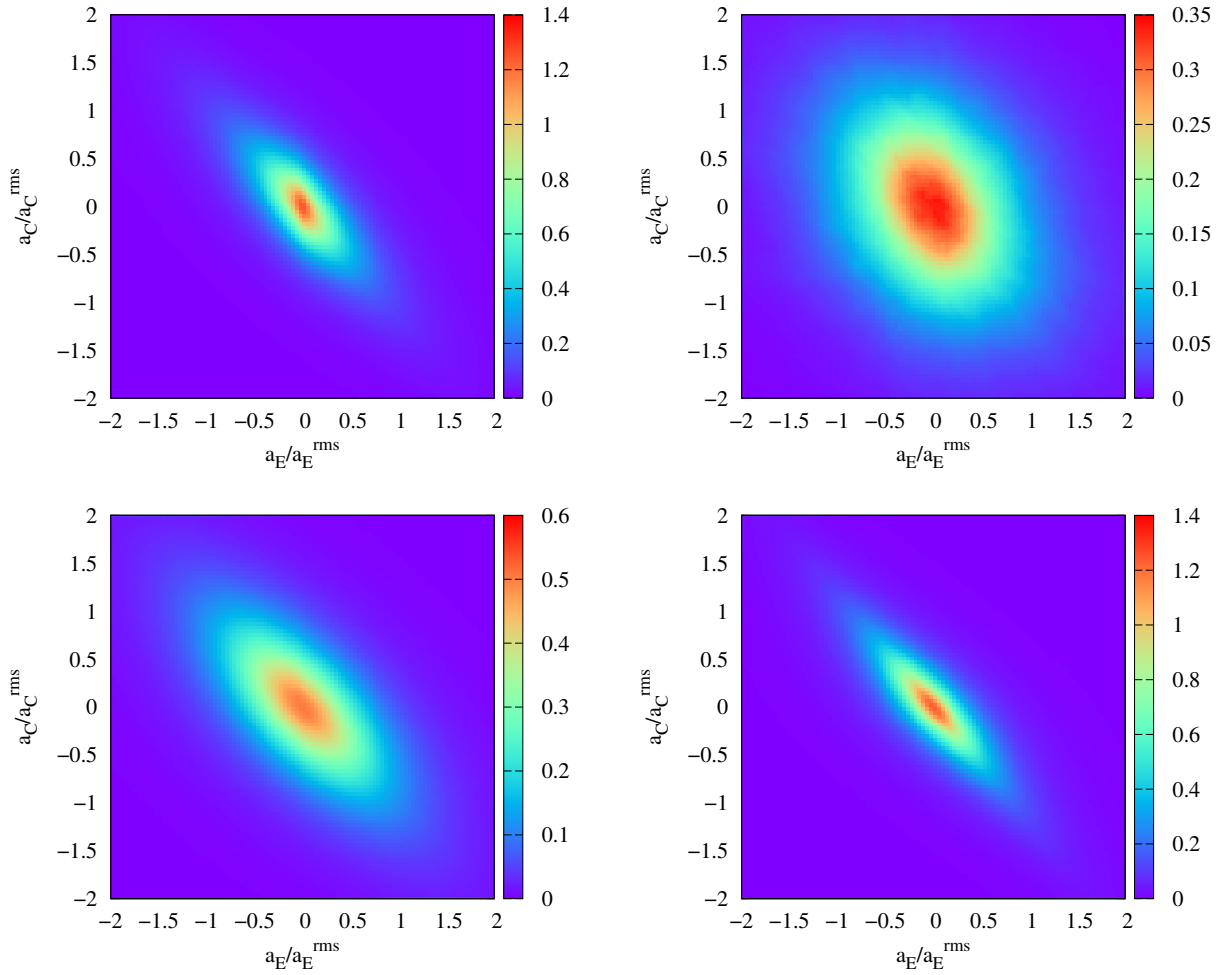

Figure 2. Joint probability distribution functions (pdfs) of the the Eulerian acceleration $\boldsymbol{a}_E$ and the convective acceleration $\boldsymbol{a}_C$ at nondimensional time $St = 10$ for the total fields (top, left) and for the decomposed fields at scales $j = 2$ (top, right), $j = 3$ (center, left), $j = 4$ (center, right), $j = 6$ (bottom, left), and $j = 8$ (bottom, right).

To understand the magnitude of the Eulerian and Lagrangian accelerations, we statistically assess, following Tsinober *et al.* (2001), the alignment properties of $\boldsymbol{a}_E$, $\boldsymbol{a}_C$, and its sum, corresponding to the Lagrangian acceleration $\boldsymbol{a}_L = \boldsymbol{a}_E + \boldsymbol{a}_C$. When the vectors of the Eulerian acceleration $\boldsymbol{a}_E$ and the convective acceleration $\boldsymbol{a}_C$ are anti-parallel, then the magnitude of the Lagrangian acceleration $\boldsymbol{a}_L$, is small compared to those of the Eulerian and convective contributions, since

$$\langle \boldsymbol{a}_L, \boldsymbol{a}_L \rangle = \langle \boldsymbol{a}_E + \boldsymbol{a}_C, \boldsymbol{a}_E + \boldsymbol{a}_C \rangle = \langle \boldsymbol{a}_E, \boldsymbol{a}_E \rangle + \langle \boldsymbol{a}_C, \boldsymbol{a}_C \rangle + 2\cos(\boldsymbol{a}_E, \boldsymbol{a}_C)\, ||\boldsymbol{a}_E||\, ||\boldsymbol{a}_C||. \quad (5)$$

Applying the wavelet decomposition to the different accelerations in eq. (2), we can study, in addition to the total, also the scale-dependent alignment properties of the Eulerian and convective accelerations, i.e., $\cos(\boldsymbol{a}_E^j, \boldsymbol{a}_C^j)$ and check its implications for the Lagrangian acceleration.

We can directly conclude that, if $\boldsymbol{a}_E^j$ and $\boldsymbol{a}_C^j$ are anti-aligned and the cosine term is negative, the norm of $\boldsymbol{a}_L^j$ becomes minimal. This means that for perfect anti-alignment Taylor's hypothesis would hold and temporal variations thus correspond to the spatial variations. Quantifying the departure of alignment yields a measure for how well Taylor's approximation holds at different scales of motion, as detailed below.

RESULTS AND DISCUSSION

Flow Evolution

Fig. 1 (left) provides the evolution of the turbulent kinetic energy $K = 1/2\langle \boldsymbol{u}, \boldsymbol{u} \rangle$ normalized by its initial value K_0. The turbulent kinetic energy initially decays due to the isotropic initial conditions, starts to grow at about $St = 2$, and eventually grows exponentially starting at about $St = 4$. The evolution equation for K can be written in the following nondimensional form:

$$\gamma = \frac{1}{SK}\frac{dK}{dt} = \frac{P}{SK} - \frac{\varepsilon}{SK} \quad (6)$$

Here, γ is the growth rate of the turbulent kinetic energy, $P/(SK)$ its normalized production rate, and $\varepsilon/(SK)$ the normalized dissipation rate. The evolution of γ, $P/(SK)$, and $-\varepsilon/(SK)$ is shown in Fig. 1 (right) and the three terms are approximately constant for $St \geq 4$. Once the normalized production and dissipation rates have reaches constant values, resulting in a constant growth rate γ, eq. (6) can be integrated to

Table 1. Pearson correlation coefficient between the Eulerian acceleration $\boldsymbol{a}_E$ and the convective acceleration $\boldsymbol{a}_C$ as a function of scale j and nondimensional time St or Taylor-microscale Reynolds number Re_λ.

St	$St=4$	$St=7$	$St=10$
Re_λ	103.43	136.40	156.90
total	-0.79688	-0.79152	-0.79612
$r(j=0)$	-0.20819	-0.48831	0.22471
$r(j=1)$	-0.01186	-0.17431	-0.23597
$r(j=2)$	-0.23966	-0.34748	-0.36848
$r(j=3)$	-0.52569	-0.55758	-0.58615
$r(j=4)$	-0.67770	-0.68890	-0.69352
$r(j=5)$	-0.75734	-0.75537	-0.75556
$r(j=6)$	-0.81143	-0.80741	-0.80288
$r(j=7)$	-0.86320	-0.86073	-0.85560
$r(j=8)$	-0.89679	-0.90279	-0.90486

obtain

$$K = K^* e^{\gamma St} \tag{7}$$

In the following, the flow is analyzed in the exponential growth regime with $St \geq 4$.

Table 2. Scale-dependent flatness of the Lagrangian acceleration Fl_{a_L} as a function of scale j and nondimensional time St or Taylor-microscale Reynolds number Re_λ.

St	$St=4$	$St=7$	$St=10$
Re_λ	103.43	136.40	156.90
total	13.47	20.77	27.81
$Fl(j=0)$	3.77	6.35	6.72
$Fl(j=1)$	3.26	3.63	3.75
$Fl(j=2)$	4.30	4.55	4.63
$Fl(j=3)$	4.79	5.38	5.93
$Fl(j=4)$	5.91	6.29	7.25
$Fl(j=5)$	8.17	10.35	12.44
$Fl(j=6)$	16.55	25.42	30.54
$Fl(j=7)$	45.81	107.90	111.72
$Fl(j=8)$	82.07	298.47	327.36

Table 3. Scale-dependent flatness of the Eulerian acceleration Fl_{a_E} as a function of scale j and nondimensional time St or Taylor-microscale Reynolds number Re_λ.

St	$St=4$	$St=7$	$St=10$
Re_λ	103.43	136.40	156.90
total	10.10	11.96	14.41
$Fl(j=0)$	3.71	5.51	5.22
$Fl(j=1)$	3.54	3.47	4.09
$Fl(j=2)$	4.35	4.36	4.72
$Fl(j=3)$	4.70	5.43	5.53
$Fl(j=4)$	5.86	6.01	6.55
$Fl(j=5)$	7.30	7.70	8.22
$Fl(j=6)$	9.69	11.35	12.45
$Fl(j=7)$	16.63	22.57	25.92
$Fl(j=8)$	32.88	47.88	56.43

Scale-Dependent Statistics

Fig. 2 provides the joint probability distribution functions (pdfs) of the Eulerian acceleration $\boldsymbol{a}_E$ and the convective acceleration $\boldsymbol{a}_C$ as a function of scale j at nondimensional time $St = 10$. While the joint pdf of the total fields (top, left) shows some negative correlation, the joint pdfs clearly become more and more negatively correlated as the scale j increases and the scale of the motion decreases.

Table 1 shows the Pearson correlation coefficient r between the Eulerian acceleration $\boldsymbol{a}_E$ and the convective acceleration $\boldsymbol{a}_C$ as a function of scale j and nondimensional time St. For all times, a negative value of $r = -0.8$ is found for the total fields. For a given time St, the value of r decreases with increasing scale index j or decreasing scale of the turbulent motion. For the smaller scales of the turbulent motion with scale index $j \geq 4$, the results obtained for r at different times St remain approximately the same. For the larger scales of the turbulent motion with scale indices $1 \leq j \leq 3$, the results for r decrease with time St and a stronger anti-alignment is observed for later times. Only the results for $j = 0$ show a different trend, but only few wavelet modes contribute to this value for r. Table 1 also gives the Taylor-microscale Reynolds number corresponding to the different times in the flow's evolution with later times corresponding to higher Reynolds numbers due to the exponential evolution of the flow.

Tables 2 and 3 provide the flatness values for the Lagrangian and Eulerian accelerations, respectively. Both the values for the total accelerations and for their scale dependence are shown. The results are presented at three nondimensional times $St = 4$, $St = 7$, and $St = 10$, corresponding to three different Reynolds numbers $Re_\lambda = 103.43$, $Re_\lambda = 136.40$, and $Re_\lambda = 156.90$. Except for the flatness values at the largest scale of motion ($j = 0$), the flatness values increase with decreasing scale of motion (or increasing j). For a given scale, the flatness values of both accelerations increase with increasing nondimensional time St and increasing Reynolds number Re_λ. While the flatness values of the total Lagragian acceleration are always larger than those of the corresponding total Eulerian acceleration, this result does not hold at all scales of

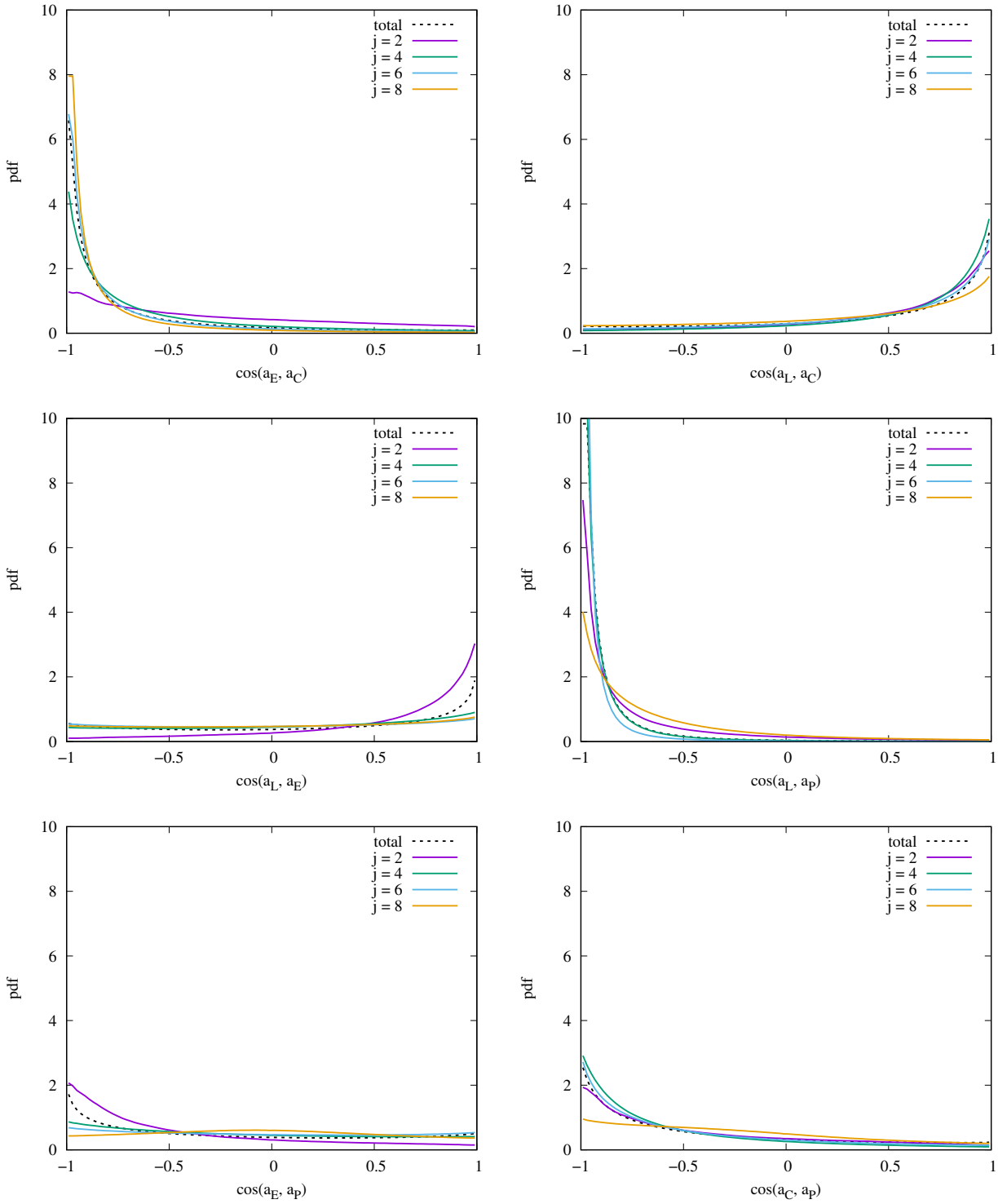

Figure 3. Probability distribution functions (pdfs) of the cosine of the angle between the Eulerian acceleration and the advection term (top, left), Lagrangian acceleration and the advection term (top, right), Lagrangian and Eulerian accelerations (center, left), Lagrangian acceleration and the pressure-gradient term (center, right), Eulerian acceleration and the pressure-gradient term (bottom, left), as well as the advection term and the pressure gradient term (bottom, right) at time $St = 10$. *Note that the pdfs are shown for the total flow fields (dashed lines), and the flow fields at the scales* $j = 2$ *(large scale), 4, 6 and 8 (small scale).*

motion. For the larger scales of the motion ($0 \leq j \leq 4$), the flatness values of the two accelerations are similar. For the smaller scales of the motion ($5 \leq j \leq 8$), the flatness values of the Lagrangian acceleration are in some cases substantially larger than the corresponding values for the Eulerian acceleration.

These observations are consistent with previous work by Yoshimatsu *et al.* (2009) considering homogeneous isotropic turbulence at a Reynolds number $Re_\lambda = 732$. It was observed that the flatness values of the Lagrangian and Eulerian ac-

celerations 'increase with scale [index] for the turbulent flow, but the flatness of the Lagrangian acceleration is one order of magnitude larger than the flatness of the Eulerian acceleration, which shows the extreme intermittency of the former.' In a comparison to random fields with phase randomization, it was found that 'the flatness remains almost constant, around 5 for the Lagrangian acceleration and around 6 for the Eulerian acceleration, which confirms that the latter yields a Laplace distribution whose flatness is 6. This proves that the random fields are non intermittent, as no scale dependence can be observed, even if their pdfs of acceleration are strongly non-Gaussian.'

Fig. 3 shows the pdf of the cosine of the angle between different vector-valued quantities for the total and scale-dependent fields for $j = 2,4,6$, and 8 (from large to small scales). The following observations can be made. The Eulerian and convective accelerations have the tendency of being strongly anti-aligned, reflected in a peak at -1 in the pdf of $\cos(\boldsymbol{a}_E,\boldsymbol{a}_c)$ (top, left). The peak is more strongly pronounced at small scales, and weak or no alignment is found at large scales. The reason for this observation is that the advection term is essentially a small scale quantity. This finding supports that Taylor's hypothesis holds at small scales in homogeneous turbulent shear flow. In contrast, for the pdf of $\cos(\boldsymbol{a}_L,\boldsymbol{a}_C)$ (top, right), we observe a slight probability for alignment, which becomes weaker at small scales. Consequently, the Langrangian and Eulerian accelerations are somewhat aligned (center, left), corresponding to a peak at $+1$ in the pdf of $\cos(\boldsymbol{a}_L,\boldsymbol{a}_E)$. This behavior becomes stronger for large scales. The reason is again that the convective term is a small scale quantity and thus supports Taylor's hypothesis.

In the pdf for $\cos(\boldsymbol{a}_L,\boldsymbol{a}_p)$ we find likewise strong anti-alignment, which is most pronounced at intermediate scales and weakens at the largest and smallest scales (center, right). The alignment of the Lagrangian acceleration and the pressure-gradient confirms the results in Jacobitz & Schneider (2021) that the pressure-gradient is the dominant term contributing to the Lagrangian acceleration. The pdf of $\cos(\boldsymbol{a}_E,\boldsymbol{a}_P)$ shows some anti-alignment, which is stronger at large scales, and no alignment is observed at small scales (bottom, left). A similar weak anti-alignment behavior is found for the pdf of $\cos(a_C,a_p)$ (bottom, right).

CONCLUSIONS

We performed direct numerical simulation in order to revisit Taylor's hypothesis in homogeneous turbulent shear flow. We found strong anti-correlation of the Eulerian acceleration with the convective acceleration based on the joint pdf and the Pearson correlation coefficient. The scale dependence of the results was studied using an orthogonal wavelet decomposition. We observed that the anti-correlation of the Eulerian acceleration and the convective acceleration is strongest for the smallest scales of the turbulent pdf the Eulerian acceleration and the convective acceleration. The pdf shows again strong anti-alignment of the terms, indicating a cancellation between the two accelerations, which is again strongest at small scales. However, this result does not hold for the largest scales of the motion. Hence, the results confirm that Taylor's hypothesis holds at small scales and not at large scales of the turbulent motion, which is in agreement with Lin (1953), who wrote that 'there is no general extension of Taylor's hypothesis to the case of shear flow.'

ACKNOWLEDGEMENTS

KS acknowledges support from Agence Nationale de la Recherche, project CM2E (ANR-20-CE46-0010-01), and the French Research Federation for Fusion Studies within the framework of the European Fusion Development Agreement (EFDA). FGJ acknowledges support from the University Professor award and the Saber3 cluster computer at the University of San Diego.

REFERENCES

Champagne, F. H., Harris, V. G. & Corrsin, S. 1970 Experiments on nearly homogeneous turbulent shear flow. *J. Fluid Mech.* **41** (1), 81–139.

Del Alamo, J. C. & Jiménez, J. 2009 Estimation of turbulent convection velocities and corrections to Taylor's approximation. *J. Fluid Mech.* **640**, 5–26.

Farge, M. & Schneider, K. 2015 Wavelet transforms and their applications to mhd and plasma turbulence: a review. *J. Plasma Phys.* **81** (6), 435810602.

He, G., Jin, G. & Yang, Y. 2017 Space-time correlations and dynamic coupling in turbulent flows. *Annu. Rev. Fluid Mech.* **49**, 51–70.

Jacobitz, F. G., Sarkar, S. & Van Atta, C. W. 1997 Direct numerical simulations of the turbulence evolution in a uniformly sheared and stably stratified flow. *J. Fluid Mech.* **342**, 231–261.

Jacobitz, F. G. & Schneider, K. 2021 Lagrangian and Eulerian accelerations in turbulent stratified shear flows. *Phys. Rev. Fluids* **6**, 074609.

Lin, C. C. 1953 On Taylors hypothesis and the acceleration terms in the Navier-Stokes equation. *Quarterly of Applied Mathematics* **10** (4), 295–306.

Moin, P. 2009 Revisiting Taylor's hypothesis. *J. Fluid Mech.* **640**, 1–4.

Pinsky, M., Khain, A. & Tsinober, A. 2000 Accelerations in isotropic and homogeneous turbulence and Taylors hypothesis. *Phys. Fluids* **12** (12), 3195–3204.

Rogallo, R. S. 1981 Numerical experiments in homogeneous turbulence. Technical Report TM 81315. NASA Ames Research Center, Moffett Field, CA, United States.

Rohr, J. J., Itsweire, E. C., Helland, K. N. & Van Atta, C. W. 1988 An investigation of the growth of turbulence in a uniform-mean-shear flow. *J. Fluid Mech.* **187**, 1–33.

Rose, W. G. 1966 Results of an attempt to generate a homogeneous turbulent shear flow. *J. Fluid Mech.* **25**, 97–120.

Salhi, A., Jacobitz, F. G., Schneider, K. & Cambon, C. 2014 Nonlinear dynamics and anisotropic structure of rotating sheared turbulence. *Phys. Rev. E* **89**, 013020.

Schneider, K., Farge, M. & Kevlahan, N. 2004 Spatial intermittency in two–dimensional turbulence: a wavelet approach. In *Woods Hole Mathematics, Perspectives in Mathematics and Physics*, pp. 302–328. World Scientific.

Taylor, G. I. 1938 The spectrum of turbulence. *Proceedings of the Royal Society of London. Series A-Mathematical and Physical Sciences* **164** (919), 476–490.

Tennekes, H. 1975 Eulerian and Lagrangian time microscales in isotropic turbulence. *J. Fluid Mech.* **67** (3), 561–567.

Tsinober, A., Vedula, P. & Yeung, P.K. 2001 Random Taylor hypothesis and the behavior of local and convective accelerations in isotropic turbulence. *Phys. Fluids* **13** (7), 1974–1984.

Yoshimatsu, K., Okamoto, N., Schneider, K., Kaneda, Y. & Farge, M. 2009 Intermittency and scale-dependent statistics in fully developed turbulence. *Phys. Rev. E* **79** (2), 026303.